Available online at www.sciencedirect.com
ScienceDirect
Geochimica et Cosmochimica Acta 71 (2007) 1087–1097
Geochimica
www.elsevier.com/locate/gca

Modeling the composition of the pore water in a clay-rock geological formation (Callovo-Oxfordian, France)

P. Leroy [a,b], A. Revil [a,*], S. Altmann [b], C. Tournassat [c]

[a] CNRS-CEREGE, Département d'Hydrogéophysique et Milieux Poreux, Université Paul Cézanne, Aix-en-Provence, France
[b] ANDRA, 1-7 rue Jean Monnet, 92298 Chatenay-Malabry, France
[c] BRGM, 3 avenue C. Guillemin, BP 6009, 45061 Orléans, France

Received 21 July 2006; accepted in revised form 7 November 2006

Abstract

The interstitial water contained in the microporosity of highly compact clay-rich media does not obey the classical condition usually used to derive the ionic composition of a solution. This is because the requirement for global electroneutrality of a charged microporous body (one having a significant fraction of pores with dimensions of the same order of size as the diffuse double layer) implies that the net charge density of the pore water must balance the deficiency (or the excess) of electrical charge carried by the solid matrix. In order to determine the solution composition in the micropores of a clay-rock, we first generalize the Donnan equilibrium conditions for the case of a multi-ionic electrolyte, with partitioning of the charge compensating counterions between the Stern and the diffuse layers A material-specific geochemical equilibrium model, incorporating an electrical triple layer model for adsorption reactions, is used to calculate the partition coefficient for the compensating ion charge (i.e., the fraction of charge in the Stern layer). This is then used to calculate the osmotic pressure and ionic composition of the pore water in the micropores. The material considered in this study is the argillite clay-rock sampled from the Callovo-Oxfordian geological formation under consideration in France for a deep geological disposal facility for radioactive waste.

1. Introduction

The chemical composition of the pore water in compacted clay-rich porous media influences both their swelling properties and the diffusion of the ions through their connected porosity (e.g., Ochs et al., 2001; Loret et al., 2004). A portion of the Callovo-Oxfordian (argillite) formation located in the eastern part of the Paris Basin in France has been the target of many scientific investigations over the past decade (e.g., Gaucher et al., 2004; Gonçalves et al., 2004; ANDRA, 2005; Revil et al., 2005 and references therein) to determine its capacity to act as a host rock for a deep geological disposal facility for radioactive wastes. These investigations are supervised by ANDRA, the French agency for nuclear waste management. The recovery of representative pore water samples from these types of rocks is almost impossible due to their very low permeability ($\sim 10^{-21}$ m^2) and low water content, but also because commonly applied techniques such as high pressure squeezing can introduce experimental and analytical artefacts (Sacchi et al., 2000).

These problems have led such research scientists as Bradbury and Baeyens (1998) and Beaucaire et al. (2000) to propose thermodynamic models for calculating the pore water chemistry for other clay-rich geological formations, respectively the Opalinus Clay (Switzerland) and the Boom Clay (Belgium) formations. A similar type of model, called THERMOAR, has been developed by Gaucher et al. (2006) to calculate the pore water chemistry of the Callovo-Oxfordian formation. Although this model was designed to estimate the composition of the 'mobile' water which would be sampled by in situ experiments, the current version does not contain an electrical double layer model

* Corresponding author.
E-mail address: revil@cerege.fr (A. Revil).

0016-7037/$ - see front matter © 2006 Elsevier Inc. All rights reserved.
doi:10.1016/j.gca.2006.11.009

for ion distribution at charged interfaces, which is needed to account for the effect of 'exclusion' of anions from the immobile water adjacent to clay mineral surfaces, i.e., in the vicinity of the shear plane (Fig. 1). To compensate for this, a correction factor was introduced. The value of this factor was taken to be on the order of 0.5 based on knowledge of the wetted surface area to pore volume ratio, the number of adsorbed water layers on clay mineral surfaces and a reasonable thickness for a diffuse layer (ANDRA, 2005; Gaucher et al., 2006). The THERMOAR model therefore can be considered to calculate the composition of the solution far from mineral surfaces, i.e., that of "macropores" within the rock or in a solution reservoir in equilibrium with a clay-rock under in situ conditions.

In the Callovo-Oxfordian argillites, most of the connected pores are associated with clay minerals and have characteristic dimensions in the 2–50 nm range (Sammartino et al., 2003). The mineralogy of the argillites can be subdivided into three mineral groups (Sammartino et al., 2003): a tectosilicate group (mainly quartz and some feldspars), a carbonate group (mainly calcite and some dolomite), and a phyllosilicate group (illite/smectite mixed layers and non-swelling minerals: kaolinite, mica, chlorite). The mineral with the highest specific surface area is the smectite and therefore, the chemical reactions controlling the exchange of ions will be principally those associated with this mineral. Smectite minerals have a permanent negative structural charge on their basal planes due to isomorphic substitution, as well as amphoteric edge sites (ANDRA, 2005). In the following we will consider that the connected microporosity is principally bounded by the basal planes of these minerals (i.e., that the amphoteric sites on the clay platelet edges do not effect the solution composition). We will also not consider the pore solution contained within the clay interlayer spaces since these spaces are too small for diffuse layer development and were assumed to contain only charge compensating cations (i.e., anions are completely excluded, neglecting the effect of ion pair exchange at the considered ionic strengths, Tournassat et al., 2004).

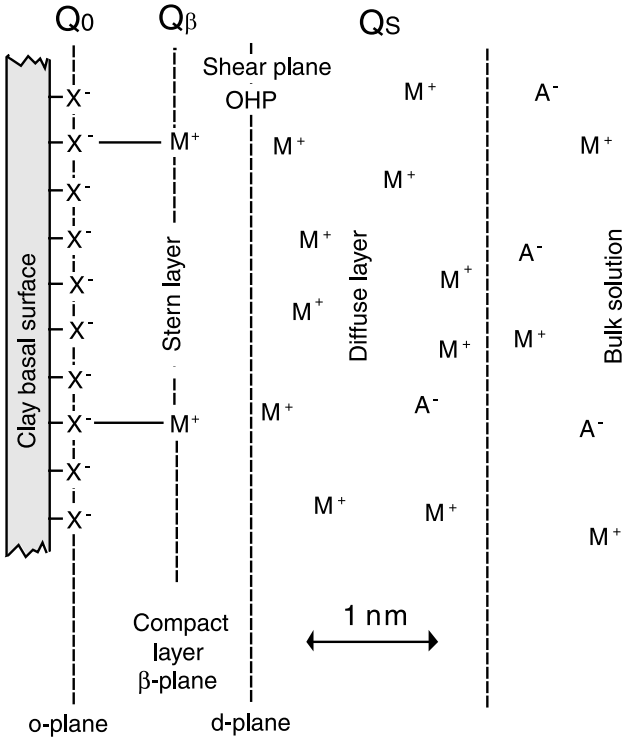

Fig. 1. Sketch of the electrical triple layer model at the clay basal surface in the case of a binary monovalent electrolyte, M represents the metal cations (e.g., Na^+) and A the anions (e.g., Cl^-). OHP represents the Outer Helmholtz Plane (*d*-plane), which coincides here with the shear plane along which the zeta potential is defined. The *β*-plane corresponds to the mean plane of the Stern layer while the *o*-plane corresponds to the surface of the basal plane.

The ionic distribution in the micropore solution is influenced by the negative charge excess on the clay mineral basal planes, i.e., an excess of cations (and deficit of anions) in the adjacent pore water (e.g., Ochs et al., 2004). The resulting ionic imbalance will have a particularly strong effect on the mean solution composition of the interstitial water contained in small dimension pores (the microporosity), i.e., the mean solution composition will not obey the classical electroneutrality condition. Ochs et al. (2004) modeled the pore water chemistry of bentonite at different total porosities (material bulk densities) recognizing the influence of the diffuse layer upon the concentration of the ionic species in the porosity. Bourg et al. (2003) have characterized the variation in pore size categories (macro, meso, interlayer) in bentonite—solution systems as a function of material density, and modeled the effects on water and ion diffusion within the material. There does not exist, however, to the best of our knowledge, a thermodynamic model capable of calculating the ionic composition of a charged porous media wherein the pore space available for coupled anion–cation transport is considered as made up of two pore size classes, macropores and micropores, with the cut-off characteristic dimension being determined by that of the diffuse layer thickness.

In this paper, we (i) extend the Donnan equilibrium condition to cover the case of a multi-ionic electrolyte and use it to calculate the ionic activities in the micropores as a function of the ionic activities in the macropores, and (ii) use a material-specific geochemical equilibrium model, incorporating an electrical triple layer model for adsorption reactions, to calculate the partitioning of counterions in the micropores between the Stern and diffuse layers. The Stern layer is a layer of sorbed counterions in contact with the charged basal surfaces of the clay minerals, while the diffuse layer of counterions and co-ions extends outwards into solution (see Fig. 1b). In addition, we determine the osmotic pressure within the Callovo-Oxfordian porosity based on the ionic concentrations in the macropores and micropores. Finally, we calculate the mean total concentration of species i in the pore space, accounting for the relative contributions of the two pore size classes.

2. Description of the porous medium

We consider a charged porous medium made up of two pore size classes—i.e., micro and macropores. Here we will use the term microporosity to describe the fraction of the connected porosity with a pore size below a length characterizing the extension into solution of the diffuse layer. The size of the diffuse layer is controlled by the Debye screening length, which depends on the ionic strength of the pore water in the macropores or in a reservoir of ions in contact with the sediment (Hunter, 1981). The fraction of the porosity considered as microporosity will therefore depend on the ionic strength of the pore water of an ionic reservoir locally in contact, and in thermodynamic equilibrium, with the charged porous medium. In the following, ϕ (dimensionless) denotes the total connected porosity, denotes the microporosity, and denotes the macroporosity (i.e., $\phi = \phi_m + \phi_p$). To determine the composition of the pore water, we consider the pore water as a three-phase medium comprising: (i) the interface between the pore water and the surfaces of the minerals represented in terms of a triple layer-based surface complexation and speciation model, (ii) the microporosity, characterized by a deficiency of co-ions and excess of counterions, and (iii) the macropores, characterized by a classical electroneutrality condition. In addition, we consider the porous medium as a closed system at thermodynamic equilibrium.

3. Generalized Donnan equilibrium model

We assume that thermodynamic equilibrium holds between the water located in the microporosity and the water contained into the macroporosity. The electrochemical potentials of the water solvent and dissolved cation and anion species are:

$$\hat{\mu}_w^p = \hat{\mu}_w^{R,p} + k_b T \ln a_w^p + \Omega_w p_p, \quad (1)$$

$$\hat{\mu}_w^m = \hat{\mu}_w^{R,m} + k_b T \ln a_w^m + \Omega_w p_m, \quad (2)$$

$$\hat{\mu}_i^p = \hat{\mu}_i^{R,p} + k_b T \ln a_i^p, \quad (3)$$

$$\hat{\mu}_i^m = \hat{\mu}_i^{R,m} + k_b T \ln a_i^m + q_i \varphi_m, \quad (4)$$

where the superscripts "m" and "p" refer respectively to the pore fluid inside the microporosity and the macroporosity of the charged medium, the superscript R refers to a stress-free reference state, which is necessarily a thermostatic state. We note as φ_m the mean electrical potential inside the pores of the charged material, a_w and a_i denote the activities of water and of the ionic species i, k_b is the Boltzmann constant (1.381×10^{-23} J K^{-1}), $q_i = (\pm e) z_i$ is the charge of species i of valence z_i, e represents the elementary charge (positive, 1.6×10^{-19} C), Ω_w and p denote the specific molar volume of water (in m^3) and the pore fluid pressure (in Pa), respectively, and T represents the absolute temperature (in K). We have neglected the partial pressure and gravity terms in the expression of the effective chemicopotentials of the component i embedded in the pore water.

Equilibrium states are states for which the dissipation function is zero. This yields the equality of all the thermodynamic potentials between the microporosity and the macroporosity of the system,

$$\hat{\mu}_w^p = \hat{\mu}_w^m, \quad (5)$$

$$\hat{\mu}_w^{R,p} = \hat{\mu}_w^{R,m}, \quad (6)$$

$$\hat{\mu}_i^p = \hat{\mu}_i^m, \quad (7)$$

$$\hat{\mu}_i^{R,p} = \hat{\mu}_i^{R,m}. \quad (8)$$

These conditions are the so-called Donnan equilibrium conditions. In addition to the equilibrium conditions, we also specify the equations for species and charge conservation. Considering Q types of ions in the pore water, this yields,

$$\Omega_w C_w^m + \sum_{i=1}^{Q} \Omega_i C_i^m = 1, \quad (9)$$

$$\Omega_w C_w^p + \sum_{i=1}^{Q} \Omega_i C_i^p = 1, \quad (10)$$

$$\sum_{i=1}^{Q} q_i C_i^m = \overline{Q}_V^m, \quad (11)$$

$$\sum_{i=1}^{Q} q_i C_i^p = 0, \quad (12)$$

where C_i and C_w are the concentrations of the ions of species i and water, respectively (the concentrations are expressed in mol m^{-3} in S.I. units but expressed below, for convenience, in mol L^{-1}), $\overline{Q}_V^m$ is the volumetric charge density in the microporosity (in C m^{-3}), and Ω_i the specific molar volume of species i (expressed in m^3 mol^{-1}). The volumetric charge density is defined by,

$$\overline{Q}_V^m = (1 - f_Q) Q_V^m, \quad (13)$$

where f_Q is the fraction of counterions located in the Stern layer or, in other words, the partition coefficient of the counterions between the Stern and the diffuse layers. Its value will be calculated by the triple layer-based surface complexation model developed in Section 4. The parameter Q_V^m represents the total bulk charge density corresponding to the excess of charge per unit pore volume of the porous material.

For clay-rich media, the total bulk charge density is calculated by (e.g., Revil et al., 2002 and references therein),

$$Q_V^m = \rho_g \left(\frac{1 - \phi}{\phi} \right) \mathrm{CEC}, \quad (14)$$

where ρ_g is the grain density (in kg m^{-3}), ϕ is the connected porosity, and CEC is the cation exchange capacity of the medium (in meq g^{-1}). According to Eqs. (1), (2), (5), (6), (9), and (10), and assuming (i) that the activity coefficient of water can be approximated by its concentration and (ii) that only solutes present outside the Stern layer

influence the electrochemical potential of the water solvent, the osmotic pressure in the microporosity is given by,

$$\pi_m = p_m - p_p, \tag{15}$$

$$\pi_m = \frac{k_b T}{\Omega_w} \ln\left(\frac{C_w^p}{C_w^m}\right), \tag{16}$$

$$\pi_m = \frac{k_b T}{\Omega_w} \ln\left(1 + \frac{C_w^p - C_w^m}{C_w^m}\right), \tag{17}$$

$$\pi_m \approx \frac{k_b T}{\Omega_w} \sum_{i=1}^{Q} \Omega_i (C_i^m - C_i^p), \tag{18}$$

where we have used the approximation $\Omega_w C_w^m \approx 1$. Eq. (18) is the van't Hoff equation. Using Eqs. (3), (4), (7), and (8) yields the Boltzmann distribution for the activities inside the micropores,

$$a_i^m = a_i^p \exp\left(-\frac{q_i \varphi_m}{k_b T}\right). \tag{19}$$

The ionic activity depends on the product of the activity coefficient and the ionic concentration. This implies respectively for micropores and macropores that:

$$a_i^m = \gamma_i^m C_i^m, \tag{20}$$

$$a_i^p = \gamma_i^p C_i^p, \tag{21}$$

where γ_i is the activity coefficient of species i (calculated in this paper by the Davies equation). In the case of the Callovo-Oxfordian argillite, we consider that the activity coefficient in the micropores is similar to the activity coefficient in the macropores (see the Appendix A),

$$\gamma_i^m \approx \gamma_i^p, \tag{22}$$

According to Eqs. (18)–(22) the osmotic pressure in the micropores is,

$$\pi_m \approx k_b T \sum_{i=1}^{Q} C_i^p \left[\exp\left(-\frac{q_i \varphi_m}{k_b T}\right) - 1\right]. \tag{23}$$

Using Eqs. (11), (19), (20), (21), and (22), we can show that the volumetric charge density is related to the electrical potential φ_m by,

$$\overline{Q}_V^m \approx \sum_{i=1}^{Q} q_i C_i^p \exp\left(-\frac{q_i \varphi_m}{k_b T}\right). \tag{24}$$

Eq. (24) establishes a useful relationship between the electrical potential φ_m and the volumetric charge density $\overline{Q}_V^m$, which can be determined from a triple layer model and the values of the ionic concentrations in the macropores. For small potentials $\overline{Q}_V^m$, such that $|\varphi_m| \ll k_b T/e$ ($k_b T/e \approx 25.7$ mV at 25 °C), we can use asymptotic developments which yield, after simple algebraic manipulations,

$$\varphi_m \approx -\frac{k_b T}{2 I_p e^2} \overline{Q}_V^m, \tag{25}$$

$$I_p \equiv \frac{1}{2} \sum_{i=1}^{Q} \left(\frac{q_i}{e}\right)^2 C_i^p, \tag{26}$$

where I_p is the ionic strength of the pore water contained in the macropores (in mol L^{-1}). For example, with $I_p = 10^{-1}$ mol L^{-1} and $\overline{Q}_V^m = 5 \times 10^6$ C m^{-3}, we obtain φ_m (25 °C) = −7 mV. However, these first-order approximations cannot be used to determine the electrical potential in the micropores in the case of the Callovo-Oxfordian argillite. They can, on the other hand, be used to determine, using an iterative procedure, the exact values of the charge density and electrical potential in the pore water. In Section 5, we will need a second-order approximation to calculate the electrical potential in the micropores. This second-order approximation is obtained by solving the second-order Eq. (24), yielding:

$$-\frac{2e^2 I_p}{k_b T} \varphi_m + \left(\sum_{i=1}^{Q} \frac{q_i^3 C_i^p}{2(k_b T)^2}\right) \varphi_m^2 - \overline{Q}_V^m = 0. \tag{27}$$

To determine the partition coefficient entering into Eq. (13), we need a triple layer model for the solid-solution interface of the clay minerals in contact with the pore solution. Such a model is developed in the next section.

4. Electrical triple layer model

In order to determine the chemical composition of a solution in equilibrium with a material such as the Callovo-Oxfordian argillite (see Section 5), it is necessary to model the effects of exchange reactions that occur at the surface of the mineral grains. Electrical triple layer models (e.g., Avena and De Pauli, 1998; Revil and Leroy, 2001; Leroy and Revil, 2004) of solute species reactions with the charged sites on clay mineral basal planes allow calculation of counter and co-ion distribution between the Stern layer and Gouy-Chapman diffuse layer (e.g., Ochs et al., 2001). Such a model was developed for the Callovo-Oxfordian argillites.

4.1. The argillite TLM model

The electrical triple layer model (TLM) we developed to model co- and counterion distribution at the basal plane/water interface of smectitic clay minerals makes several simplifying assumptions. First we assume that the amphoteric groups on the smectite edges do not contribute to the co- and counterion distributions between the Stern and diffuse layers in the microporosity. This is justified primarily by the fact that pore water pH of the Callovo-Oxfordian formation is near neutral (Gaucher et al., 2006) and, under these conditions, the charge density induced by edge sites is likely to be small relative to that due to permanent excess of negative charge created by the isomorphic substitutions inside the crystalline network of the smectite (e.g., Tournassat et al., 2004).

We therefore consider only these latter sites in the model which we will represent as "X sites" (one negative charge per site: X^-). The mineral surface charge density Q_0 (in C m^{-2}) associated with these sites is considered equal to the ratio between the cation exchange capacity (CEC) of smectite (1 meq g^{-1}) and its specific surface (800 m^2 g^{-1}, see Revil et al. (1998) and references therein), which gives a value equal to 0.75 charge nm^{-2}.

The surface charge density Q_0 for the clay minerals in the Callovo-Oxfordian argillite in equilibrium with a contacting solution phase can then be expressed as follows:

$$Q_0 = -e(\Gamma^0_{X} + 2\Gamma^0_{X_2Ca} + 2\Gamma^0_{X_2Mg} + \Gamma^0_{XNa} + \Gamma^0_{XK}), \tag{28}$$

where Γ^0_i is the surface site density of species i (in sites m^{-2}). The surface charge density Q_β in the Stern layer is determined according to:

$$Q_\beta = e(2\Gamma^0_{X_2Ca} + 2\Gamma^0_{X_2Mg} + \Gamma^0_{XNa} + \Gamma^0_{XK} + \Gamma^0_{XH}). \tag{29}$$

The surface charge density in the diffuse layer is calculated in the case of a multi-component electrolyte (Hunter, 1981):

$$Q_S = \left\{ 2\varepsilon k_b T \sum_{i=1}^{Q} C_i^p \left[\exp\left(-\frac{q_i \varphi_d}{k_b T} \right) - 1 \right] \right\}^{1/2}, \tag{30}$$

where ε is the dielectric permittivity of the fluid at the mineral/water interface. We consider here that the permittivity ε is equal to its value for the bulk water ($\varepsilon_f \approx 81\varepsilon_0$; $\varepsilon_0 \approx 8.85 \times 10^{-12}$ F m^{-1}). We did not use the ionic activities in Eq. (30) because we suppose that the activity coefficient in the macropores is roughly equal to the activity coefficient in the micropores (see the Appendix A). The electrical potential φ_d (in V) is that of the Outer Helmholtz Plane (see OHP on Fig. 1). We make the assumption that φ_d is equal to the zeta potential ζ measured on clay particles; this potential is assumed to be that existing at the particle electrokinetic shear plane (where the relative velocity between the grains and the electrolyte is null). The zeta potential is a key potential to model electrokinetic properties of porous media and colloidal suspensions under non-equilibrium thermodynamic conditions.

A simple one site model is chosen to simulate the reactions between cation species and the smectite surface in order to calculate the surface site density of each species. The reactions are written in the form of half-reactions for introduction in the TLM model framework. For monovalent cation sorption like Na^+ on these sites,

$$> XNa \Longleftrightarrow\ > X^- + Na^+,\ K_{Na}. \tag{31}$$

The symbol ">" refers to the mineral framework and K_{Na} is the associated selectivity coefficient. For divalent cation sorption like Ca^{2+} on these sites

$$> X_2Ca \Longleftrightarrow 2 > X^- + Ca^{2+},\ K_{Ca}. \tag{32}$$

The activity of the $>X_2Ca$ and the $>X^-$ sites are $a_{X_2Ca} = 2\Gamma^0_{X_2Ca}/(-Q_0/e)$ and $a_{X^-} = \Gamma^0_{X^-}/(-Q_0/e)$, respectively, using the Gaines–Thomas convention. The associated selectivity coefficient K_{Na} and K_{Ca} are expressed as a function of their equivalent fraction on the surface (Appelo and Postma, 1999):

$$K_{Na} = \frac{\Gamma^0_X(a^p_{Na^+})}{\Gamma^0_{XNa}} \exp\left(-\frac{e\varphi_\beta}{k_b T} \right), \tag{33}$$

$$K_{Ca} = -\frac{e\Gamma^{0^2}_X(a^p_{Ca^{2+}})}{2Q_0\Gamma^0_{X_2Ca}} \exp\left(-\frac{2e\varphi_\beta}{k_b T} \right). \tag{34}$$

Combining these two equations, one obtains:

$$> 2XNa + Ca^{2+} \Longleftrightarrow\ > X_2Ca + 2Na^+,\ K_{NaCa}, \tag{35}$$

with,

$$K_{NaCa} = \frac{K^2_{Na}}{K_{Ca}} = \frac{-\frac{Q_0}{e}(a^p_{Na^+})^2 2\Gamma^0_{X_2Ca}}{(a^p_{Ca^{2+}})\Gamma^{0^2}_{XNa}}. \tag{36}$$

K_{NaCa} is equivalent to the selectivity coefficient of the Na/Ca exchange in the Gaines and Thomas convention (Gaines and Thomas, 1953), providing that the value of Γ^0_X is small as compared to Q_0 in absolute value. It is therefore possible to use the exchange reactions and associated selectivity coefficients of the THERMOAR model (see Table 1; Gaucher et al., 2006), in order to obtain the half-reactions presented in Table 2. Thanks to these Gaines–Thomas exchange selectivity coefficients, we need only the value of the selectivity coefficients of the half-reaction concerning the sodium to calculate all of the other half-reactions. It is worth pointing out that the use of half-reactions and a TLM model to represent cation reactions with the permanent charge sites means that a certain fraction of the X^- sites will not be associated with counterions located in the Stern layer, which distinguishes this representation from that of classical cation exchange models.

Table 1
Speciation constants for the various cations

Chemical reaction	Gaines and Thomas selectivity coefficients
$> XNa + K^+ \Longleftrightarrow\ > XK + Na^+$	$K_{KNa} = 2.78 \pm 0.12$
$> XNa + H^+ \Longleftrightarrow\ > XH + Na^+$	$K_{HNa} = 13.00 \pm 2.63$
$2 > XNa + Mg^{2+} \Longleftrightarrow\ > X_2Mg + 2Na^+$	$K_{MgNa} = 2.41 \pm 0.09$
$2 > XNa + Ca^{2+} \Longleftrightarrow\ > X_2Ca + 2Na^+$	$K_{CaNa} = 3.17 \pm 0.10$

pH 7.3, $T = 25$ °C (one site model, from Gaucher et al., 2006, ">" refers to the mineral framework).

Table 2
Speciation constants for the various cations (half-reactions)

Half-reactions	Speciation contants
$> XNa \Longleftrightarrow\ > X^- + Na^+$	K_{Na}
$> XH \Longleftrightarrow\ > X^- + H^+$	$K_H = K_{Na}/K_{HNa}$
$> XK \Longleftrightarrow\ > X^- + K^+$	$K_K = K_{Na}/K_{KNa}$
$> X_2Ca \Longleftrightarrow 2 > X^- + Ca^{2+}$	$K_{Ca} = K^2_{Na}/K_{CaNa}$
$> X_2Mg \Longleftrightarrow 2 > X^- + Mg^{2+}$	$K_{Mg} = K^2_{Na}/K_{MgNa}$

pH 7.3, $T = 25$ °C (one site model).

We use the equilibrium constants associated with the half-reactions to calculate the surface site densities. This yields:

$$\Gamma^0_{X_2Ca} = \frac{\Gamma^{0^2}_X (a^p_{Ca^{2+}})}{-\frac{Q_0}{e} 2K_{Ca}} \exp\left(-\frac{2e\varphi_\beta}{k_b T}\right), \quad (37)$$

$$\Gamma^0_{X_2Mg} = \frac{\Gamma^{0^2}_X (a^p_{Mg^{2+}})}{-\frac{Q_0}{e} 2K_{Mg}} \exp\left(-\frac{2e\varphi_\beta}{k_b T}\right), \quad (38)$$

$$\Gamma^0_{XNa} = \frac{\Gamma^0_X (a^p_{Na^+})}{K_{Na}} \exp\left(-\frac{e\varphi_\beta}{k_b T}\right), \quad (39)$$

$$\Gamma^0_{XK} = \frac{\Gamma^0_X (a^p_{K^+})}{K_K} \exp\left(-\frac{e\varphi_\beta}{k_b T}\right), \quad (40)$$

$$\Gamma^0_{XH} = \frac{\Gamma^0_X (a^p_{H^+})}{K_H} \exp\left(-\frac{e\varphi_\beta}{k_b T}\right), \quad (41)$$

where φ_β is the electrical potential at the Stern layer plane (Fig. 1b).

By replacing Eqs. (37)–(41) in Eq. (28), we obtain a second degree equation for the surface site density of X sites, Γ^0_X:

$$\frac{Q_0}{e} + \Gamma^0_X \left[1 + \frac{a^p_{Na^+}}{K_{Na}} \exp\left(-\frac{e\varphi_\beta}{k_b T}\right) + \frac{a^p_{K^+}}{K_K} \exp\left(-\frac{e\varphi_\beta}{k_b T}\right) + \frac{a^p_{H^+}}{K_H} \exp\left(-\frac{e\varphi_\beta}{k_b T}\right)\right] + 2\Gamma^{0^2}_X \left[\frac{a^p_{Ca^{2+}}}{-\frac{Q_0}{e} 2K_{Ca}} \exp\left(-\frac{2e\varphi_\beta}{k_b T}\right) + \frac{a^p_{Mg^{2+}}}{-\frac{Q_0}{e} 2K_{Mg}} \exp\left(-\frac{2e\varphi_\beta}{k_b T}\right)\right] = 0. \quad (42)$$

This equation was used to compute the surface density of X sites as a function of the electrical potential at the Stern layer, β plane (Fig. 1b). Using Eqs. (37)–(41), the surface site densities can be expressed as a function of the electrical potential on the β plane.

The global electroneutrality equation for the TLM model is,

$$Q_0 + Q_\beta + Q_S = 0. \quad (43)$$

The electrical potentials at the surface of the clay minerals, φ_0, at the β plane, φ_β, and at the Outer Helmholtz Plane, φ_d, are related by a series capacitor model, which is a classical approach in the context of the TLM theory (e.g., Persello, 2002),

$$\varphi_0 - \varphi_\beta = Q_0/C_1, \quad (44)$$

$$\varphi_\beta - \varphi_d = -Q_S/C_2. \quad (45)$$

The parameters C_1 and C_2 (in F m^{-2}) are the (constant) integral capacitances of the inner and outer parts of the Stern layer, respectively. We calculate the potential φ_d using Eqs. (28)–(45). Finally, we need to optimize only three parameters, the capacitances C_1 and C_2 and the equilibrium constant associated with the sodium complexation half-reaction, K_{Na}.

4.2. Comparison with experimental data

The previously described forward model is set up as a Matlab® routine (Fig. 2). We use the Simplex algorithm (Caceci and Cacheris, 1984) to optimize the parameters of our model to fit the experimental data. The algorithm minimizes the following cost function R:

$$R^2 = \frac{\sum_{i=1}^N \omega_i \left(\zeta^i_{Mes} - \zeta^i_{Model}\right)^2}{N \sum_{i=1}^N \omega_i}, \quad (46)$$

where ζ^i_{Mes} and ζ^i_{Model} are, respectively, the experimentally determined zeta potential (determined by electrophoresis or streaming current measurements) and the zeta potential calculated by the TLM model. The coefficients ω_i are the statistical weights given to the measurements i depending on their standard deviations; they are taken as equal to 1 here.

We decided to optimize only the equilibrium constant K_{Na} because sensitivity analyses show that the value of the capacitance C_1 does not significantly influence the calculation of the potential φ_d (see Leroy and Revil, 2004). In the literature, the value of the capacitance C_2, for a number of minerals, is taken as constant and usually equal to 0.2 F m^{-2} (Gutierrez and Fuentes, 1996; Kitamura et al., 1999; Persello, 2002).

We start the optimization with an a priori model that was chosen randomly in a range of a priori potential range of values for the model parameters (null a priori information for this range corresponds to a random choice). We then determined the mean and standard deviation of the optimized model parameter using a Monte-Carlo procedure. As explained above, we have only one parameter in our model to optimize: K_{Na}. We use an a priori density probability corresponding to the null information in the range $K_{Na} \in [10^{-2}; 1]$. The zeta potentials were taken from measurements of colloidal suspensions of Na, Ca, Mg Montmorillonite in NaCl, $CaCl_2$, $MgCl_2$ electrolytes,

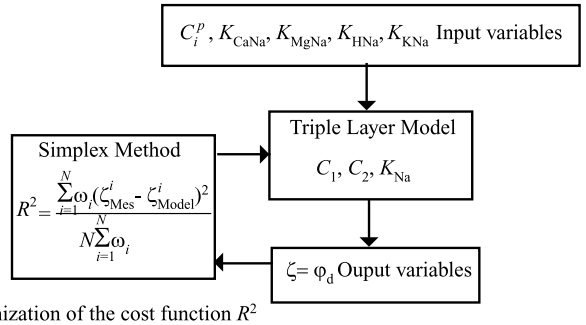

Fig. 2. Sketch of the optimization procedure. A Matlab routine is used to determine the zeta potential of smectite as a function of the type of counterions using the Gaines–Thomas selectivity coefficients and the equilibrium constant associated with the adsorption of sodium. The other parameters, the capacities C_1 and C_2 are not optimized. Their values are taken from Avena and De Pauli (1996), Gutierrez and Fuentes (1996), Kitamura et al. (1999), and Persello (2002).

respectively taken from Sondi et al. (1996) and Rosanne et al. (2003). These authors use Henry's equation to relate the electrophoretic mobility and the zeta potential, which implies that they do not account in their measurements for the influence of surface conductivity. Neglecting surface conductivity leads to under estimation of the zeta potential values (Revil et al., 1999, 2002; Perrier and Froidefond, 2003). This explains why we test our model only with the experimental data obtained at high salinities (10^{-1} mol L^{-1} in the present case) for which the influence of surface conductivity can be considered as negligible. However the measured values of the zeta potential should be considered as lower bounds for the real values of the inner-potential of the diffuse layer.

We found that the predictions of the model are in relatively good agreement with the experimental data for Na^+, Ca^{2+}, and Mg^{2+} counterions (see Fig. 3). For each type of counterion, we use the half-reaction corresponding to its adsorption reaction. The optimized parameter of the equilibrium constant K_{Na} is equal to 0.8 ± 0.5. Within the calculated uncertainty, the estimated K_{Na} is essentially the same as Avena and De Pauli (1998) ($K_{Na} = 0.77$).

4.3. Calculation of the partition coefficient

Using the optimized value of the equilibrium constant K_{Na}, the electrical triple layer model is now run to determine the partition coefficient f_Q for the case of a multi-ionic electrolyte. This partition coefficient f_Q is defined as the fraction of counterions located in the Stern layer:

$$f_Q = \frac{\sum_{i=1}^{Q} z_i \Gamma^0_{X_iM}}{\sum_{i=1}^{Q} z_i \Gamma^0_{X_iM} + \sum_{i=1}^{Q} z_i \Gamma^S_{X_iM}}. \quad (47)$$

The parameters $\Gamma^0_{X_iM}$ and $\Gamma^S_{X_iM}$ are respectively the surface site density of adsorbed counterions in the Stern and in the diffuse layer. The value Q is the number of types of counterions in the electrolyte. The surface site density of adsorbed counterions in the diffuse layer is given by integrating the excess of the concentration of counterions in the diffuse layer. This yields

$$\Gamma^S_{X_iM} = C_i^p \int_0^{2\chi_d} \left\{ \exp\left[-\frac{q_i \varphi(x)}{k_b T} \right] - 1 \right\} dx, \quad (48)$$

where x is the distance taken locally extending from the smooth surface of the mineral (in m) and χ_d (in m) is the Debye length. The electrical potential $\varphi(x)$ is calculated by the expression,

$$\varphi(x) = \varphi_d \exp(-x/\chi_d). \quad (49)$$

By using Eqs. (47)–(49) and Eqs. (37)–(41), we obtain a value of f_Q in the range 0.94 ± 0.02, corresponding to $K_{Na} = 0.8 \pm 0.5$. This means that $94 \pm 2\%$ of the charge of the counterions are located in the Stern layer. Table 3 presents the distribution of the surface site densities of adsorbed counterions in the Stern and in the diffuse layer with $f_Q = 0.94$ (same values with $f_Q = 0.92$ and $f_Q = 0.96$). This distribution is relatively similar to the distribution of the surface sites of adsorbed cations calculated by THERMOAR using the values of the cation exchange capacity of each cation (Gaucher et al., 2006). However, the proportions of adsorbed monovalent and divalent cations in our study are respectively higher and lower than the values determined by Gaucher et al. (2006).

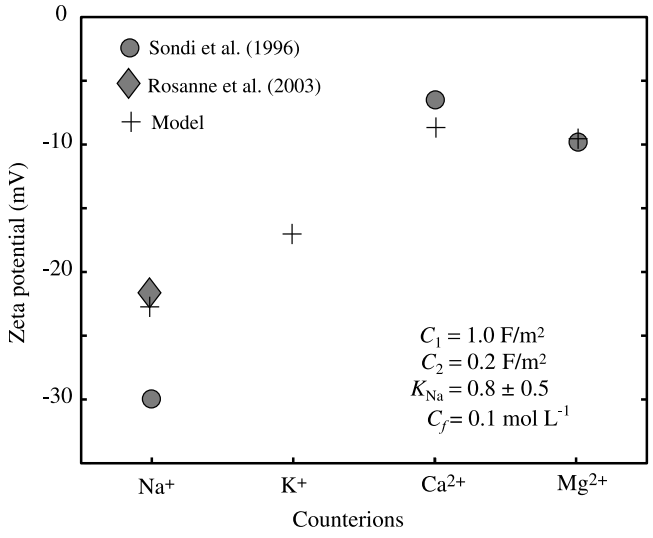

Fig. 3. Zeta potentials of colloidal suspensions of Na, K, Ca, Mg Montmorillonite in NaCl, KCl, $CaCl_2$, $MgCl_2$ electrolytes, respectively. The salinity C_f is equal to 0.1 mol L^{-1}.

Table 3
Distribution of surface site densities of adsorbed counterions in the Stern and diffuse layer ($f_Q = 0.94$) for the Callovo-Oxfordian shale

Γ_{XNa} (%)	Γ_{XK} (%)	Γ_{XH} (%)	Γ_{X_2Ca} (%)	Γ_{X_2Mg} (%)
27[a]	14.5[a]	5×10^{-6}[a]	35[a]	23[a]
14.5[b]	8.5[b]	—	47[b]	29[b]

This distribution is nearly independent of the value of the partition coefficient f_Q.
[a] Using the triple layer model developed in this paper.
[b] Gaucher et al. (2006).

5. Determination of the ionic concentrations

The model developed above allows calculation of the composition of the pore water in the micropores as a function of the composition of the pore water in the macropores. As a first approximation, the macropore solute composition is considered to be that calculated by the THERMOAR model (Gaucher et al., 2006). The total Na, Ca, K, Mg, Cl, S (in sulphate form) concentrations, and solution pH are given in Table 4 for a simplified water composition, i.e., neglecting minor species such as Sr, Si, Al, and Fe species. The speciation of the solution was determined using the code PHREEQC v2.12 and the Llnl.dat database (see Parkhurst and Appelo, 1999). Table 4 also gives the major solute species concentrations (minor species are considered as those whose mole fraction is

Table 4
Ionic concentrations in the macropores of the Callovo-Oxfordian shale

THERMOAR model (Gaucher et al., 2006)		PHREEQC2 speciation calculation (major species)		Simplified macropore solute composition (only charged species)	
Species	C_i^p (in mol L^{-1})	Species	C_i^p (in mol L^{-1})	Species	C_i^p (in mol L^{-1})
Na	32×10^{-3}	Na^+	31.8×10^{-3}	Na^+	31.5×10^{-3}
K	7×10^{-3}	K^+	6.7×10^{-3}	K^+	6.5×10^{-3}
Ca	15×10^{-3}	Ca^{2+}	9.7×10^{-3}	Ca^{2+}	9.5×10^{-3}
		$CaSO_4$	5.2×10^{-3}	—	—
Mg	14×10^{-3}	Mg^{2+}	8.4×10^{-3}	Mg^{2+}	8.1×10^{-3}
		$MgSO_4$	5.6×10^{-3}	—	—
Cl	30×10^{-3}	Cl^-	30×10^{-3}	Cl^-	30×10^{-3}
S(+6)	34×10^{-3}	SO_4^{2-}	20.6×10^{-3}	SO_4^{2-}	21×10^{-3}
pH	7.3	H^+	6.1×10^{-8}	—	—
		OH^-	2.7×10^{-7}	—	—
pCO_2	−2.5	HCO_3^-	1.2×10^{-3}	HCO_3^-	1.2×10^{-3}

below 10% of the total element concentration). The solute species are mainly the dissociated cations and anions, as well as neutral solute complexes such as $CaSO_4$ and $MgSO_4$. The value of the ionic strength determined from the code PHREEQC2 is 0.11 mol L^{-1}. This value is very similar to the experimental value used to fit the K_{Na} parameter of the TLM model. In the following, a simplified water composition (see Table 4), taking into account only the major charged species, will be used to calculate the solute composition of the micropore solution. The concentrations have been adjusted slightly to satisfy the electroneutrality of the simplified macropore solution.

The volumetric charge density in the micropores was calculated using the value of the partition coefficient and the concentrations of the ions in the macropores. Using the values of the cation exchange capacity, the porosity, and the grain density reported in Table 5, with $f_Q = 0.94$, we obtain ($\overline{Q}_V^m = 1.43\times10^7$ C m^{-3}, $\varphi_m = -17.7$ mV). We found ($\overline{Q}_V^m = 1.91\times10^7$ C m^{-3}, $\varphi_m = -23.8$ mV) and ($\overline{Q}_V^m = 9.54\times10^6$ C m^{-3}, $\varphi_m = -11.6$ mV) with $f_Q = 0.92$ and $f_Q = 0.96$, respectively. From Eqs. (19)–(22) and the values of the mean potential in the microporosity φ_m, we determined the concentrations of the ions in the micropores, which are reported in Table 6. The ionic activities in the macropores are calculated according to the values of the ionic concentrations in the macropores presented in Table 6 and using Eq. (21) and the Davies equation. We used the value of the electrical potential in the micropores, the values of the ionic activities in the macropores, and Eq. (19) to determine the ionic activities in the micropores. These ionic activities are reported in Table 7.

Table 5
Properties of the Callovo-Oxfordian argillite

Symbols	Meaning	Value
ϕ	Connected porosity	0.164 ± 0.018[a]
f_m	Fraction of microporosity	0.50[c]
ρ (kg m^{-3})	Bulk density	2420 ± 30[b]
ρ_g (kg m^{-3})	Grain density	2700[c]
CEC (meq g^{-1})	Cation exchange capacity	0.18 ± 0.05[d]
φ_W	Clay fraction	0.45 ± 0.05[a]

[a] ANDRA (2005).
[b] We use $\rho = (1-\phi)\,\rho_g + \phi\rho_f$.
[c] This study.
[d] Gaucher et al., 2004, Hole EST205, excluding the strongly calcareous beds.

Table 7
Activities of the ionic species in the macropores and in the micropores of the Callovo-Oxfordian shale

Species	a_i^p	a_i^m ($f_Q = 0.92$)	a_i^m ($f_Q = 0.94$)	a_i^m ($f_Q = 0.96$)
Na^+	2.45×10^{-2}	6.19×10^{-2}	4.87×10^{-2}	3.86×10^{-2}
K^+	5.06×10^{-3}	1.28×10^{-2}	1.06×10^{-2}	7.96×10^{-3}
H^+	3.90×10^{-8}	9.85×10^{-8}	7.75×10^{-8}	6.14×10^{-8}
Ca^{2+}	3.50×10^{-3}	2.23×10^{-2}	1.38×10^{-2}	8.64×10^{-3}
Mg^{2+}	2.98×10^{-3}	1.90×10^{-2}	1.18×10^{-2}	7.37×10^{-3}
Cl^-	2.34×10^{-2}	9.26×10^{-3}	1.18×10^{-2}	1.49×10^{-2}
SO_4^{2-}	7.73×10^{-3}	1.21×10^{-3}	1.96×10^{-3}	3.13×10^{-3}
HCO_3^-	9.35×10^{-4}	3.70×10^{-4}	4.71×10^{-4}	5.94×10^{-4}

Table 6
Concentrations of the ionic species in the macropores and in the micropores of the Callovo-Oxfordian shale

Species	C_i^p in mol L^{-1}	$C_i^m(f_Q = 0.92)$ in mol L^{-1}	$C_i^m(f_Q = 0.94)$ in mol L^{-1}	$C_i^m(f_Q = 0.96)$ in mol L^{-1}
Na^+	3.15×10^{-2}	7.95×10^{-2}	6.26×10^{-2}	4.95×10^{-2}
K^+	6.50×10^{-3}	1.64×10^{-2}	1.29×10^{-2}	1.02×10^{-2}
H^+	5.01×10^{-8}	1.26×10^{-7}	9.95×10^{-8}	7.88×10^{-8}
Ca^{2+}	9.50×10^{-3}	6.05×10^{-2}	3.75×10^{-2}	2.35×10^{-2}
Mg^{2+}	8.10×10^{-3}	5.16×10^{-2}	3.20×10^{-2}	2.00×10^{-2}
Cl^-	3.00×10^{-2}	1.19×10^{-2}	1.51×10^{-2}	1.91×10^{-2}
SO_4^{2-}	2.10×10^{-2}	3.30×10^{-3}	5.32×10^{-3}	8.50×10^{-3}
HCO_3^-	1.20×10^{-3}	4.76×10^{-4}	6.04×10^{-4}	7.63×10^{-4}

Finally, we calculated the osmotic pressure in the Callovo-Oxfordian porosity using Eq. (18). Using $f_Q = 0.94$, we obtained $\pi_0 = 144$ kPa, with values of $\pi_0 = 287$ kPa being obtained for $f_Q = 0.92$ and $\pi_0 = 59$ kPa for $f_Q = 0.96$. The values of the excess pore pressure measured within the Callovo-Oxfordian formation are in the range of 200–500 kPa (Gonçalves et al., 2004; ANDRA, 2005). The understanding of the in situ excess pore fluid pressure of the Callovo-Oxfordian formation clearly deserves further attention.

Finally, the total concentration of species i in the pore space of the porous material is given by the sum of the concentrations in the micro and macroporosity weighted by the volumetric fractions of each porosity,

$$C_i = f_m C_i^m + (1 - f_m) C_i^p, \tag{50}$$

where f_m is the volumetric fraction of the microporosity relative to the total porosity. Using Eqs. (19)–(22) together with Eq. (50) yields a relationship between the total concentration of species i and the concentration of the same ionic species in the macropores, C_i^p, and the mean electrical potential in the micropores φ_m,

$$C_i = [1 - f_m(1 - \vartheta_m)] C_i^p, \tag{51}$$

$$\vartheta_m \equiv \exp\left(-\frac{q_i \varphi_m}{k_b T}\right). \tag{52}$$

To evaluate the fraction of the micropores, f_m, we need to evaluate the size of the Stern and of the diffuse layer. The minimum size of the Stern layer corresponds to the mean diameter of hydrated cations. Their values are comprised between 1 and 2 nm (Kitamura et al., 1999). Consequently, we assume that the Stern layer is approximately 2 nm thick. Using the value of the ionic strength in the macropores, the Debye screening length that controls the thickness of the diffuse layer is close to 1 nm. The thickness of the diffuse layer is approximately twice the Debye screening length. If we define the critical size of the pores as the size used to distinguish between the microporores and the macropores, it follows that the critical size of the pore is 8 nm. Fig. 4 represents a typical pore size distribution for Callovo-Oxfordian rock (Sammartino et al., 2003; ANDRA, 2005). The mean pore size of the macroporosity is equal to 28 ± 5 nm using the distribution of Fig. 4. Consequently, using the distribution of the pore size of Fig. 4, we found $f_m = 0.5$, taking into account the diffuse layer also present on the surfaces of the macropores.

The values of the total concentration of species i and of the ionic concentration in the micropores and macropores are presented in Tables 6 and 8. The total concentration of species i is really influenced by the electrochemical properties of the mineral/water interface for all the values of the partition coefficient f_Q. The concentrations of divalent cations are much higher than their concentrations in the macropores. The concentrations of monovalent cations significantly increase and the concentration of anions decrease dramatically compared to their values in the macropores.

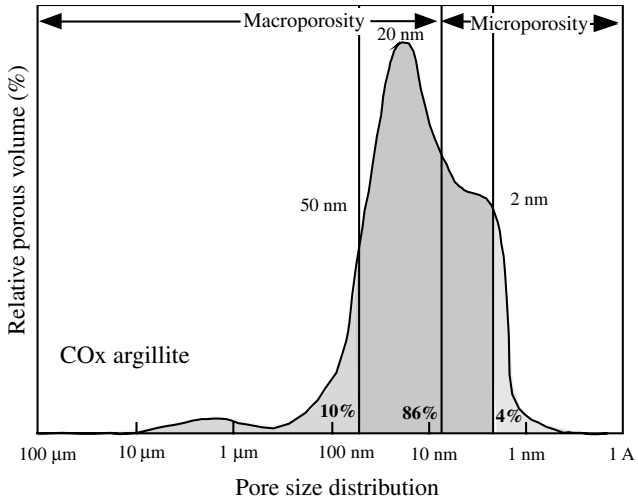

Fig. 4. Pore size distribution of the Callovo-Oxfordian argillite (from ANDRA, 2005). The distinction between the macroporosity and the microporosity is based on the thickness of the diffuse layer.

Table 8
Total concentration of the ionic species in the macropores and in the micropores for different values of the partition coefficient f_Q of the Callovo-Oxfordian shale

Species	C_i ($f_Q = 0.92$) in mol L^{-1}	C_i ($f_Q = 0.94$) in mol L^{-1}	C_i ($f_Q = 0.96$) in mol L^{-1}
Na^+	5.55×10^{-2}	4.70×10^{-2}	4.05×10^{-2}
K^+	1.14×10^{-2}	9.70×10^{-3}	8.36×10^{-3}
H^+	8.83×10^{-8}	7.48×10^{-8}	6.45×10^{-8}
Ca^{2+}	3.50×10^{-2}	2.35×10^{-2}	1.65×10^{-2}
Mg^{2+}	2.98×10^{-2}	2.00×10^{-2}	1.41×10^{-2}
Cl^-	2.09×10^{-2}	2.26×10^{-2}	2.45×10^{-2}
SO_4^{2-}	1.21×10^{-2}	1.32×10^{-2}	1.47×10^{-2}
HCO_3^-	8.38×10^{-4}	9.02×10^{-4}	9.82×10^{-4}

These total concentrations are determined from Eq. (50) with $f_m = 0.50$ for the volumetric fraction of the microporosity relative to the total porosity.

6. Concluding statements

In this paper, we have presented a method to estimate the composition of the water contained in the micropores and the bulk water contained in the macropores of clay-rich media. These types of media are being considered as host rocks for geologic repositories, and the proposed methodology addresses the difficulties of determining a representative in situ pore water chemistry. This is an important issue in geochemistry, because it is very difficult to obtain representative pore water samples for analysis from such clay-rock formations at great depths. The Callovo-Oxfordian argillite is under consideration as a host formation for deep geological disposal of high-level radioactive waste in France. Similar rock formations are under evaluation in other countries, including Belgium and Switzerland, posing similar problems. An important underlying

need when building a theory for transport of ions in porous media, especially diffusion, is a model for determining the concentrations of ionic species in the thermostatic reference state, and especially the partitioning of these species between the micropores and the macropores of porous media with a broad distribution of pore sizes. The problem is especially important in charged media because the pore water filling the microporosity does not obey the electroneutrality condition. In this paper, we solved this problem by coupling a Donnan description of equilibrium conditions with an electrical triple layer speciation model for calculating the partitioning of counterions between the Stern and the diffuse layer. We also calculated the osmotic pressure within the medium. The value we determined corresponds to the lower limit of the measured excess pressure in the Calloxo-Oxfordian formation. We found that approximately 50% of the connected porosity is affected by the excess of electrical charge at the surface of clay minerals. The concentrations of cations in the microporosity are much higher than their values in the macropores. The anionic concentrations in the micropores are much lower than their values in the macropores. We plan to use the present results to model the effective diffusivity of ions in this type of porous material using the model of Leroy et al. (2006) extended to multi-component electrolytes by Revil and Linde (2006).

Acknowledgments

This work is supported by the French National Research Council (CNRS), the GDR-FORPRO, and the French National Agency for Radioactive Waste Management (ANDRA). Joël Lancelot is strongly thanked for his support through the GDR FORPRO, respectively. The post-doctoral grant of P. Leroy is supported by ANDRA. This is a contribution FORPRO 2006-11A. We thank the AE Chen Zhu and the two referees for their very constructive comments.

Associate editor: Chen Zhu

Appendix A

The ionic strength in the micropores I_m is calculated by an expression similar to Eq. (26),

$$I_m = \frac{1}{2}\sum_{i=1}^{Q}\left(\frac{q_i}{e}\right)^2 C_i^m. \tag{A1}$$

Using Eqs. (19), (20), and (A1), we obtain,

$$I_m = \frac{1}{2}\sum_{i=1}^{Q}\left(\frac{q_i}{e}\right)^2 \frac{a_i^p}{\gamma_i^m}\exp\left(-\frac{q_i\varphi_m}{k_bT}\right). \tag{A2}$$

Davies's equation allows to determine the activity coefficient in the micropores γ_i^m of species i as a function of the ionic strength I_m ($I_m \leqslant 0.5$ mol L^{-1}),

$$\log\gamma_i^m = -0.5\left(\frac{q_i}{e}\right)^2\left(\frac{\sqrt{I_m}}{1+\sqrt{I_m}} - 0.3I_m\right). \tag{A3}$$

For small potentials φ_m, such as $\varphi_m \ll k_bT/e$, we use second-order approximations to determine the electrical potential φ_m as a function of the ionic strength I_m. Eqs. (A1)–(A3) yield

$$\begin{aligned} I_m\gamma &- \frac{2}{\gamma^3}\left(a^p_{Ca^{2+}} + a^p_{Mg^{2+}} + a^p_{SO_4^{2-}}\right) \\ &- \frac{1}{2}\left(a^p_{Na^+} + a^p_{K^+} + a^p_{H^+} + a^p_{Cl^-} + a^p_{OH^-}\right) \\ &+ \frac{e\varphi_m}{k_bT}\left[\frac{4}{\gamma^3}\left(a^p_{Ca^{2+}} + a^p_{Mg^{2+}} - a^p_{SO_4^{2-}}\right)\right. \\ &\left.+\frac{1}{2}\left(a^p_{Na^+} + a^p_{K^+} + a^p_{H^+} - a^p_{Cl^-} - a^p_{OH^-}\right)\right] \\ &+ \left(\frac{e\varphi_m}{k_bT}\right)^2\left[-\frac{4}{\gamma^3}\left(a^p_{Ca^{2+}} + a^p_{Mg^{2+}} + a^p_{SO_4^{2-}}\right)\right. \\ &\left.-\frac{1}{4}\left(a^p_{Na^+} + a^p_{K^+} + a^p_{H^+} + a^p_{Cl^-} + a^p_{OH^-}\right)\right] = 0, \end{aligned} \tag{A4}$$

$$\gamma \equiv 10^{-0.5\left(\frac{\sqrt{I_m}}{1+\sqrt{I_m}} - 0.3I_m\right)}. \tag{A5}$$

According to Eqs. (11), (19), and (20),

$$\overline{Q}_V^m = \sum_{i=1}^{Q}\frac{q_ia_i^p}{\gamma_i^m}\exp\left(-\frac{q_i\varphi_m}{k_bT}\right). \tag{A6}$$

We use a second-order approximation for the electrical potential φ_m in Eq. (A6),

$$\overline{Q}_V^m \approx \sum_{i=1}^{Q}\frac{q_ia_i^p}{\gamma_i^m}\left[1 - \frac{q_i\varphi_m}{k_bT} + 0.5\left(\frac{q_i\varphi_m}{k_bT}\right)^2\right]. \tag{A7}$$

We replace in Eq. (A7) φ_m by its expression calculated as a function of the ionic strength I_m, which is solution of Eqs. (A4) and (A5), and we replace γ_i^m by its expression given according to Davies's equation, Eq. (A3). We found an equation with the unknown I_m and we use the gradient's method to determine this parameter. We obtain $I_m = 0.3$ mol L^{-1}. According to Davies's equation, (A3), the activity coefficient does not change dramatically with the ionic strength. Consequently, if the ionic strengths of the pore waters in the macropores and in the micropores are quite similar, and we can assume that,

$$\gamma_i^m \approx \gamma_i^p. \tag{A8}$$

Poisson's equation allows determination of the electrostatic potential in the micropores φ_m resulting from the volumetric charge density $\overline{Q}_V^m$ by solving,

$$\nabla^2\varphi_m = -\frac{\overline{Q}_V^m}{\varepsilon_f}. \tag{A9}$$

By combining Eqs. (11), (20), and (A9), we obtain,

$$\nabla^2\varphi_m = -\sum_{i=1}^{Q}\frac{q_i}{\varepsilon_f}\frac{a_i^m}{\gamma_i^m}. \tag{A10}$$

By inserting Eq. (19) into Eq. (A10) and using Eq. (22), we found,

$$\nabla^2\varphi_m \approx -\sum_{i=1}^{Q}\frac{q_i}{\varepsilon_f}\frac{a_i^p}{\gamma_i^p}\exp\left(-\frac{q_i\varphi_m}{k_bT}\right), \quad \text{(A11)}$$

$$\nabla^2\varphi_m \approx -\sum_{i=1}^{Q}\frac{q_i}{\varepsilon_f}C_i^p\exp\left(-\frac{q_i\varphi_m}{k_bT}\right), \quad \text{(A12)}$$

which corresponds to the classical Poisson–Boltzmann equation. The surface charge density in the diffuse layer is determined using Eq. (A12) for small values of φ_m (see Hunter, 1981).

References

ANDRA, 2005. Dossier 2005 argile—Référentiel du site de Meuse/Haute Marne, Internal Report ANDRA n°C.RP.ADS.04.0022.

Appelo, C.A.J., Postma, D., 1999. A consistent model for surface complexation on birnessite ($-MnO_2$) ant its application to a column experiment. *Geochim. Cosmochim. Acta* **63**, 3039–3048.

Avena, M.J., De Pauli, C.P., 1996. Modeling the interfacial properties of an amorphous aluminosilicate dispersed in aqueous NaCl solutions. *Colloids Surf.* **118**, 75–87.

Avena, M.J., De Pauli, C.P., 1998. Proton adsorption and electrokinetics of an Argentinean montmorillonite. *J. Colloid Interface Sci.* **202**, 195–204.

Beaucaire, C., Pitsch, H., Toulhoat, P., Motellier, S., Louvat, D., 2000. Regional fluid characterization and modelling of water rock equilibria in the Boom clay formation and in the Rupelian aquifer at Mol, Belgium. *Appl. Geochem.* **15**, 667–686.

Bourg, I.C., Bourg, A.C.M., Sposito, G., 2003. Modeling diffusion and adsorption in compacted bentonite: a critical review. *J. Contam. Hydrol.* **61**, 293–302.

Bradbury, M.H., Baeyens, B., 1998. A physicochemical characterisation and geochemical modeling approach for determining porewater chemistries in argillaceous rock. *Geochim. Cosmochim. Acta* **62** (5), 783–795.

Caceci, M., Cacheris, W.P., 1984. Fitting curves to data. The simplex algorithm is the answer. *Byte* **9**, 340–362.

Gaines, G.L., Thomas, H.C., 1953. Adsorption studies on clay minerals, II.A formulation of the thermodynamics of exchange adsorption. *J. Chem. Phys.* **21**, 714–718.

Gaucher, E., Robelin, C., Matray, J.M., Negrel, G., Gros, Y., Heitz, J.F., Vinsot, A., Rebours, H., Cassabagnere, A., Bouchet, A., 2004. ANDRA underground research laboratory: interpretation of the mineralogical and geochemical data acquired in the Callovo-Oxfordian Formation by investigative drilling. *Phys. Chem. Earth* **29**, 55–77.

Gaucher, E., Blanc, P., Barot, F., Braibant, G., Buschaert, S., Crouzet, C., Gautier, A., Girard, J.P., Jacquot, E., Lassin, A., Negrel, G., Tournassat, C., Vinsot, A., Altmann, S., 2006. Modeling the porewater chemistry of the Callovo-Oxfordian formation at a regional scale. *Compte Rendus Géosciences* **338** (12–13), 917–930.

Gonçalves, J., Violette, S., Wendling, J., 2004. Analytical and numerical solutions for alternative overpressuring processes: application to the Callovo-Oxfordian sedimentary sequence in the Paris Basin, France. *J. Geophys. Res.* **109**, B02110. doi:10.1029/2002JB002278.

Gutierrez, M., Fuentes, H.R., 1996. A mechanistic modeling of montmorillonite contamination by cesium sorption. *Appl. Clay Sci.* **11** (1), 11–24.

Hunter, R.J., 1981. *Zeta Potential in Colloid Science: Principles and Applications*. Academic Press, New York.

Kitamura, A., Fujiwara, K., Yamamoto, T., Nishikawa, S., Moriyama, H., 1999. Mechanism of Adsorption of cations onto quartz. *J. Nucl. Sci. Technol.* **36**, 1167–1175.

Leroy, P., Revil, A., 2004. A triple-layer model of the surface electrochemical properties of clay minerals. *J. Colloid Interface Sci.* **270** (2), 371–380.

Leroy, P., Revil, A., Coelho, D., 2006. Diffusion of ionic species in bentonite. *J. Colloid Interface Sci.* **296** (1), 248–255.

Loret, B., Gajo, A., Simões, F.M.F., 2004. A note on the dissipation due to generalized diffusion with electro-chemo-mechanical couplings in heteroionic clays. *Eur. J. Mech. A/Solid* **23**, 763–782.

Ochs, M., Lothenbach, B., Wanner, H., Sato, H., Yui, M., 2001. An integrated sorption–diffusion model for the calculation of consistent distribution and diffusion coefficients in compacted bentonite. *J. Contam. Hydrol.* **47**, 281–296.

Ochs, M., Lothenbach, B., Shibata, M., Yui, M., 2004. Thermodynamic modeling and sensitivity analysis of porewater chemistry in compacted bentonite. *Phys. Chem. Earth* **29**, 129–136.

Parkhurst, D.L., Appelo, C.A.J., 1999. User's guide to phreeqc—a computer program for speciation, batch-reaction, one-dimensional transport, and inverse geochemical calculations, U.S. Geological Survey, Report-99-4259.

Perrier, F., Froidefond, T., 2003. Electrical conductivity and streaming potential coefficient in a moderately alkaline lava series. *Earth Planet. Sci. Lett.* **210** (1–2), 351–363.

Persello, J., 2002. In: Delgado, A.V. (Ed.), *Interfacial Electrokinetics and Electrophoresis*, *Surf. Sci. Ser.*, vol. 106. Dekker, New York, p. 297.

Revil, A., Cathles, L.M., Losh, S., Nunn, J.A., 1998. Electrical conductivity in shaly sands with geophysical applications. *J. Geophys. Res.* **103** (B10), 23925–23936.

Revil, A., Schwaeger, H., Cathles, L.M., Manhardt, P., 1999. Streaming potential in porous media. 2. Theory and application to geothermal systems. *J. Geophys. Res.* **104** (B9), 20033–20048.

Revil, A., Leroy, P., 2001. Hydroelectric coupling in a clayey material. *Geophys. Res. Lett.* **28** (8), 1643–1646.

Revil, A., Hermitte, D., Spangenberg, E., Cochémé, J.J., 2002. Electrical properties of zeolitized volcaniclastic materials. *J. Geophys. Res.* **107** (B8), 2168. doi:10.1029/2001JB000599.

Revil, A., Leroy, P., Titov, K., 2005. Characterization of transport properties of argillaceous sediments. Application to the Callovo-Oxfordian Argillite. *J. Geophys. Res.* **110**, B06202. doi:10.1029/2004JB003442.

Revil, A., Linde, N., 2006. Chemico-electromechanical coupling in microporous media. *J. Colloid Interface Sci.* **302**, 682–694.

Rosanne, M., Mammar, N., Koudina, N., Prunet-Foch, B., Thovert, J.-F., Tevissen, E., Adler, P.M., 2003. Transport properties of compact clays II. Diffusion. *J. Colloid Interface Sci.* **260**, 195–203.

Sacchi, E., Michelot, J.-L., Pitsch, H., 2000. Porewater Extraction from Argillaceous Rocks for Geochemical Characterization. Methods and Interpretation. Report 66 2000 02. OECD/NEA.

Sammartino, S., Bouchet, A., Prêt, D., Parneix, J.-C., Tevissen, E., 2003. Spatial distribution of porosity and minerals in clay rocks from the Callovo-Oxfordian formation (Meuse/Haute-Marne, Eastern France)-implications on ionic species diffusion and rock sorption capability. *Appl. Clay Sci.* **23**, 157–166.

Sondi, I., Biscan, J., Pravdic, V., 1996. Electrokinetics of pure clay minerals revisited. *J. Colloid Interface Sci.* **178**, 514–522.

Tournassat, C., Ferrage, E., Poinsignon, C., Charlet, L., 2004. The titration of clay minerals. Part II. Structural-based model and implications for clay reactivity. *J. Colloid Interface Sci.* **273**, 234–246.